RSC Advances

PAPER

View Article Online
View Journal | View Issue



Cite this: *RSC Adv.*, 2020, **10**, 37456

# A comparison of experimental and theoretical studies of benzoquinone modified poly(thiophene): effect of polymerization techniques on the structure and properties†

Neetika Singh,[a] Sumit Singh,[a] Prabhat Kumar[b] and Ufana Riaz *[a]

The present manuscript reports the synthesis of benzoquinone (BQ) modified polythiophene (PTh) by chemical and microwave-assisted polymerization techniques. The synthesized oligomers were investigated for their spectral, morphological and thermal properties *via* FTIR, UV-visible, scanning electron microscopy (SEM) and thermogravimetric (TGA) analyses. Theoretical calculations were performed by using Gaussian 09 software *via* the DFT/B3LYP method with the 6-311G basis set. FTIR confirmed the formation of hydroquinone modified PTh when the polymerization was carried out by magnetic stirring and ultrasonication, while the formation of BQ modified PTh was obtained by microwave irradiation. The electronic transitions obtained *via* experimental UV-visible studies were also found to be in close agreement with the theoretical spectra. SEM revealed a well-formed morphology comprising needle shaped rods for the oligomer synthesized under microwave irradiation. The TGA-DTA studies revealed low char content for the above oligomer, while the florescence studies revealed intense emission around 450 nm. The highest quantum yield was found to be 0.024, which also showed high singlet oxygen generation tendency as well as a high single oxygen quantum yield of 0.30 and could be utilized to design imaging probes applicable in photodynamic therapy.

Received 8th September 2020
Accepted 3rd October 2020

DOI: 10.1039/d0ra07714c

rsc.li/rsc-advances



## Introduction

Conjugated polymers have been extensively investigated for their opto-electronic properties and find potential application in electro-chromic displays,[1] light-emitting devices,[2] integrated circuits,[3] sensors[4] and solar cells.[5] The electronic properties and the charge transport phenomena can be easily tailored *via* the introduction of donor/acceptor molecules and hence, these polymers have been the subject of intense investigation over the past few decades.[6] The redox behaviour of quinones and their derivatives have attracted significant attention; however, it has been scarcely explored in combination with heterocyclic conjugated polymers.[7] Several authors have reported the polymerization of polyanthraquinones and poly(*p*-benzoquinone) through organometallic polycondensation reactions.[8,9] Various results have been reported, based on the mode of synthesis of donor–acceptor polymers and the mechanism of polymerization, but the details regarding the control of the structure as well as morphology resulting from the synthetic conditions are still unexplored, and they are not well-explained even by computational studies. Hence, with the aim to investigate the influence of polymerization conditions on the electronic structure, opto-electronic properties as well as the morphology of donor–acceptor polymers, the present work reports π-conjugated oligomers composed of thiophene (acceptor) and benzoquinone (donor) units synthesized by different chemical polymerization methods: magnetic stirring, ultrasonication and microwave irradiation. Thiophene was chosen as an acceptor moiety due to its remarkable electro-chromic and optoelectronic properties, which have been scarcely investigated in combination with benzoquinone.[10–12] The chemical and physical properties of the synthesized oligomers were studied by experimental as well as theoretical IR, UV-visible spectroscopy, while the morphology was explored by the SEM studies. The thermal properties were determined by TGA-DTA analysis and the singlet oxygen generation studies were carried out in order to establish the potential application of these polymers in photodynamic therapy.

[a]*Materials Research Laboratory Department of Chemistry, Jamia Millia Islamia, New Delhi-110025, India. E-mail: ufana2002@yahoo.co.in*

[b]*Advance Instrumentation Research Facility, Jawaharlal Nehru University, New Delhi-110067, India*

† Electronic supplementary information (ESI) available. See DOI: 10.1039/d0ra07714c

## Experimental

### Materials and methods

Thiophene (Loba Chemie Pvt. Ltd, India), 1,4-benzoquinone (Sigma Aldrich, USA), ferric chloride ($FeCl_3 \cdot 6H_2O$) (Sd Fine

Chem Pvt. Ltd., India), chloroform ($CHCl_3$) (Merck, India) palladium acetate (Merck, India) tetrahydrofuran (THF) (Merck, India), methanol ($CH_3OH$) (Merck, India), and distilled water were used without further purification.

### Polymerization of thiophene with benzoquinone *via* chemical oxidant method by magnetic stirring and ultrasonication

Thiophene (10 ml, 0.118 mol) and 1, 4 benzoquinone (5 g, 0.046 mol) were added to an Erlenmeyer flask containing 50 ml of $CHCl_3$. The mixture was stirred with a magnetic stirrer at room temperature and ferric chloride (5 g) was added to the above solution after which there was a purge of $N_2$ gas in the above reaction. The reaction mixture switched to black color indicating polymerization of the two moieties. The reaction was further stirred on a magnetic stirrer at a temperature between 0–5 °C for 4 h and kept overnight in a deep freezer. The product was washed several times with distilled water by centrifugation and dried in a vacuum oven at 72 °C in order to ensure the removal of impurities and water. The obtained polymer was designated as PTh/BQ-MS. Similar procedure was adopted for the polymerization of thiophene with 1,4-benzoquinone by ultrasound-assisted technique and the polymer was designated as PTh/BQ-US.

### Polymerization of thiophene with benzoquinone by Suzuki reaction *via* microwave irradiation method

Thiophene (10 ml, 0.118 mol) and 1, 4 benzoquinone (5 g, 0.046 mol) were added to an Erlenmeyer flask containing 50 ml of THF. The mixture was stirred for 5 min at 25 °C. Then, the polymerization was started by injecting a solution of $Pd(IPr)(OAc)_2$ (0.05 ml, 0.02 M in THF). The reaction was subjected to microwave irradiation for 20 min at 25 °C. The polymer obtained was purified by precipitation from methanol solvent. The polymer was then collected by filtration and dried in a vacuum oven at 70 °C. The polymer obtained was designated as PTh/BQ-MW.

## Characterization

### Spectral studies

IR spectra of polymers were taken on a Shimadzu spectrophotometer Model IRA Affinity-1 in the form of KBr pellets. UV-vis spectra were taken on a UV-vis spectrophotometer (Shimadzu, Model UV-1800).

### Morphological studies

Scanning electron micrographs (SEM) were recorded on Leo Supra 50VP, Carl Zeiss scanning electron microscope. Fluorescence images were obtained by using a Laser Confocal Microscope with Fluorescence Correlation Spectroscopy (FCS)-Olympus FluoView FV1000 equipped with a He–Ne laser and oil immersion objective. The $\lambda_{max}$ for laser excitation was 410 nm.

### Computational studies

All theoretical calculations were computed by using the Gaussian 09 package. Optimizations of PTh/BQ geometries were carried out without symmetry constraints by using hybrid functional DFT/B3LYP method with 6-311G basis set.[13–15] The geometric optimization was carried out by taking 3 units of thiophene, coupled with 3 units of benzoquinone/hydroquinone. The frequency calculations (IR spectra) were computed by using same method, while the electronic transitions were calculated by using the time-dependent DFT (TD-DFT) method with 6-311G basis set.

### Thermal analysis

TGA analysis of the polymers were carried out on a thermogravimetric analyser model TA/DTA 6300, EXSTAR 6000, a heating rate of 10 °C $min^{-1}$ over a temperature range of 35–800 °C under $N_2$ atmosphere was employed.

### Singlet oxygen generation studies

Singlet oxygen photo-generation was investigated by using 0.05 mM solution of 1,3-diphenylisobenzofuran (DPBF) in ethanol. The absorbance of DPBF at 410 nm was monitored by using the Shimadzu Model 1800 UV-vis spectrometer as per method reported in our previous studies.[13]

## Result and discussion

### Conformation of electronic transitions by experimental and theoretical UV-visible studies

The UV-visible spectra of PTh/BQ-US and PTh/BQ-MS, Fig. 1(a), reveals peaks at 280 nm and 450 nm, respectively corresponding

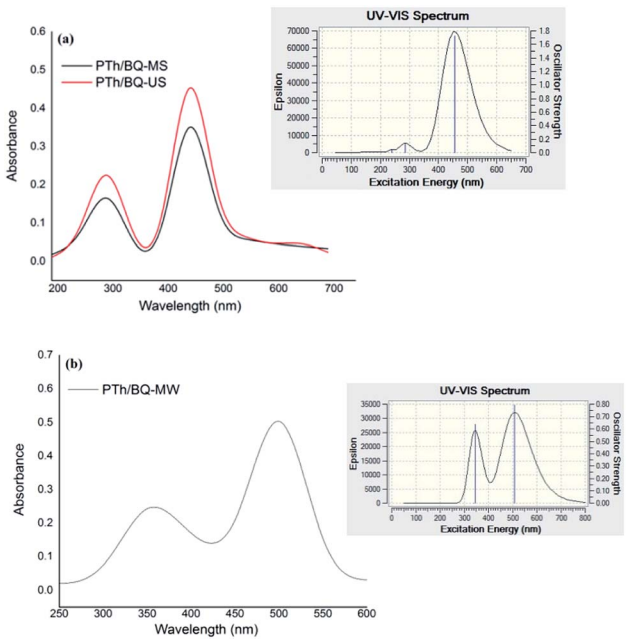


Fig. 1 UV-visible spectra of (a) PTh/BQ-MS, PTh/BQ-US and (b) PTh/BQ-MW.

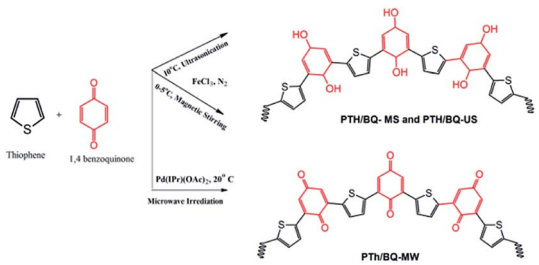


Scheme 1 Polymerization of PTh/BQ by different methods.

to π–π* of BQ and n–π* of PTh. The peak at 280 nm corresponds to the presence of hydroquinone, which was obtained when the synthesis was carried out in water medium, under magnetic stirring as well as sonication. The theoretical spectrum also reveals peaks at 286 nm and 455 nm, which were found to be in close agreement with the experimental spectra. Similarly, the UV-visible spectrum of PTh/BQ-MW, Fig. 1(b) reveals peaks at 350 nm and 500 nm, which show a major red shift of the peaks corresponding to BQ and PTh. The theoretical spectrum of the same polymer reveals peaks at 345 nm and 508 nm. Hence, it is concluded that the synthesis conditions, significantly affects the structure of BQ which is converted to hydroquinone when the polymerization is carried out under ultrasonic irradiation/magnetic stirring, while the structure of BQ is retained when the reaction is carried out under microwave irradiation *via* the Suzuki method, as shown in Scheme 1. This phenomena was further confirmed from the experimental as well as theoretical IR spectra of the oligomers.

### IR analysis of PTh/BQ-MS, PTh/BQ-US and PTh/BQ-MW

The experimental as well as the theoretical IR spectra of PTh/BQ-MS, PTh/BQ-US and PTh/BQ-MW are provided in the ESI as shown in Fig. S1(a–c).† The IR spectrum of PTh/BQ-MS, Table 1 shows the O–H stretching vibration peak at 3169 $cm^{-1}$ associated with the presence of hydroquinone, while the peak observed at 1611 $cm^{-1}$ was attributed to the C=C stretching vibration of PTh. The peaks corresponding to the benzenoid ring are observed at 1404 $cm^{-1}$ and 1321 $cm^{-1}$, respectively.[15] The C–S–C stretching vibration peak is observed at 1190 $cm^{-1}$, while the characteristic peaks at 1114 $cm^{-1}$ and 1045 $cm^{-1}$, are attributed to the aromatic OH of BQ. The absorption bands at 791 $cm^{-1}$, 786 $cm^{-1}$ and 688 $cm^{-1}$ are associated with the C–S out of the plane bending vibrations of PTh. The theoretical spectrum of the oligomer reveals the OH stretching peak at 3160 $cm^{-1}$, while the C=C stretching peak is observed at 1601 $cm^{-1}$. The C–S–C stretching vibration peak is observed at 1185 $cm^{-1}$. The aromatic OH bending peak of BQ is observed around the characteristic peaks of 1111 $cm^{-1}$, 1040 $cm^{-1}$, while the C–S out of the plane bending vibrations of PTh are observed at 793 $cm^{-1}$, 780 $cm^{-1}$ and 687 $cm^{-1}$. Likewise, the IR spectrum of PTh/BQ-US reveals an intense broad peak at 3160 $cm^{-1}$ and a shoulder at 3047 $cm^{-1}$ due to the presence of OH of hydroquinone. The C=C conjugated alkene stretching vibration peak is observed at 1640 $cm^{-1}$, while the peaks of benzenoid ring stretching vibrations are observed at 1488 $cm^{-1}$ and 1420 $cm^{-1}$ respectively. The characteristic OH peak of phenol group is observed at 1122 $cm^{-1}$, 1038 $cm^{-1}$ and the peak around 954 $cm^{-1}$ correlates with the presence of substituted benzene ring. The C–S stretching vibration peak of PTH is observed at 793 $cm^{-1}$ and 679 $cm^{-1}$. Interestingly the IR spectrum of PTh/BQ-MW reveals no peak in the OH region, thereby confirming the formation of BQ. The peaks observed at 1641 $cm^{-1}$ and 1580 $cm^{-1}$ correlate with the presence of C=C conjugated alkene of PTh. The multiple peaks observed at 1481 $cm^{-1}$, 1443 $cm^{-1}$ and 1412 $cm^{-1}$ are ascribed to the benzenoid in the BQ rings. The presence of the C–S stretching of PTh is confirmed through the absorption at 1199 $cm^{-1}$. The OH bending peak is observed at 1122 $cm^{-1}$ and 1038 $cm^{-1}$, while the peaks of the substituted benzene ring and C–S bending are observed at 954 $cm^{-1}$, 893 $cm^{-1}$ and 679 $cm^{-1}$. The above peaks confirmed the formation of PTh/BQ in different forms as shown in Scheme 1. Interestingly, the spectrum of PTh/BQ0-MW did not reveal OH stretching peak, but a small band is observed at 1720 $cm^{-1}$ which confirms the presence of carbonyl group, and is found to be absent in PTh/BQ-MS and PTh/BQ-US. Moreover, the theoretical spectrum also reveals the carbonyl peak at 1732 $cm^{-1}$. The C=C conjugated alkene stretching vibration peak is observed at 1641 $cm^{-1}$ and 1580 $cm^{-1}$, while the peaks of benzenoid ring stretching vibrations are observed at 1481 $cm^{-1}$, 1443 $cm^{-1}$ and 1412 $cm^{-1}$, respectively. The peak

Table 1 IR data of PTh/BQ-MS, PTh/BQ-US and PTh/BQ-MW

| Functional group | PTh/BQ-MS peak position exp. (theor.) $cm^{-1}$ | PTh/BQ-US exp. (theor.) $cm^{-1}$ | PTh/BQ-MW exp. (theor.) $cm^{-1}$ |
|---|---|---|---|
| O–H stretching | 3169 (3160) | 3047 (3045) | — |
| C=O stretching | — | — | 1720 (1732) |
| C=C stretching (conjugated alkene) | 1611 (1601) | 1640 (1638) | 1641 (1642), 1580 (1588) |
| C–C benzenoid | 1404 (1400) 1321 (1328) | 1488 (1481), 1420 (1418) | 1481 (1480), 1443 (1444), 1412 (1408) |
| C–O stretching | 1286 | 1283 (1285), 1235 (1243) | 1233 (1237) |
| C–S stretching | 1190 (1185) | 1199 (1194) | 1199 (1190), 1113 (1112) |
| Aromatic OH bending (phenol) | 1114 (1111), 1045 (1040) | 1122 (1117), 1038 (1033) | — |
| Substituted benzene ring and C–S bending | 791 (793), 786 (780), 688 (687) | 954 (950), 893 (893), 679 (690) | 953 (950), 844 (840), 791 (790), 693 (690) |

around 1113 $cm^{-1}$ and 1199 $cm^{-1}$ correlates with the presence of C–S stretching vibration peak, while the substituted benzene ring and C–S bending peaks are observed at 953 $cm^{-1}$, 844 $cm^{-1}$, 791 $cm^{-1}$ and 693 $cm^{-1}$. The structures of the oligomers are therefore, confirmed.

## Computational studies

The optimized structures of PTh/BQ-MS, PTH/BQ-US and PTh/BQ/MW are given in, Fig. 2(a) and (c). The C–C and C=C bond lengths for PTh/BQ-MS/US are 1.44 Å and 1.35 Å respectively, while the C–S bond length is computed to be 1.78 Å. The C–O bond length is found to be 1.36 Å. The C–C and C=C bond lengths for optimized structure of PTh/BQ/MW are computed to be 1.45 Å and 1.33 Å respectively, while the C–S and C=O bond lengths were found to be 1.80 Å and 1.21 Å, respectively. The C–S–C bond angle is computed to be 89.49°, while the C–S–C bond angle for PTH/BQ/MS/US was found to be 90.02°. The structures were noticed to be planar in both cases. The charge distribution in PTH/BQ-MS/US, Fig. 2(b) is observed to be concentrated on all carbon atoms, except the ones linked to the OH group and similar charge distribution is observed for PTh/BQ-MW, Fig. 2(d). The molecular electrostatic potential, however, is noticed to be different for the two oligomers, Fig. 2(e) and (f). For PTH/BQ-MS/US, a negative diffusion region is observed, while for PTH/BQ-MW, positive diffusion region is observed around the oligomer with positive diffusion centre around the C=O group.

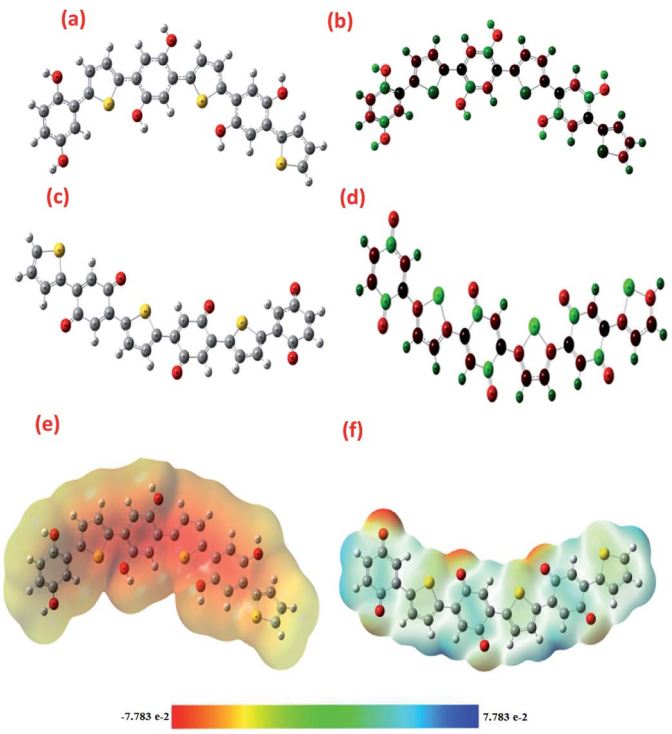


Fig. 2 (a) Optimized geometry of PTh/BQ/MS/US, (b) Mulliken charge distribution in PTh/BQ/MS/US, (c) optimized geometry of PTh/BQ/MW, (d) Mulliken charge distribution in PTh/BQ/MW, (e) molecular electrostatic potential (MEP) in PTh/BQ/MS/US, (f) molecular electrostatic potential (MEP) in PTh/BQ/MW.

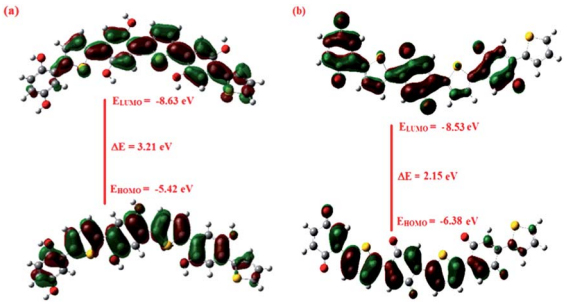


Fig. 3 Frontier molecular orbitals and band gap of (a) PTh/BQ-MS/US, (b) PTh/BQ-MW.

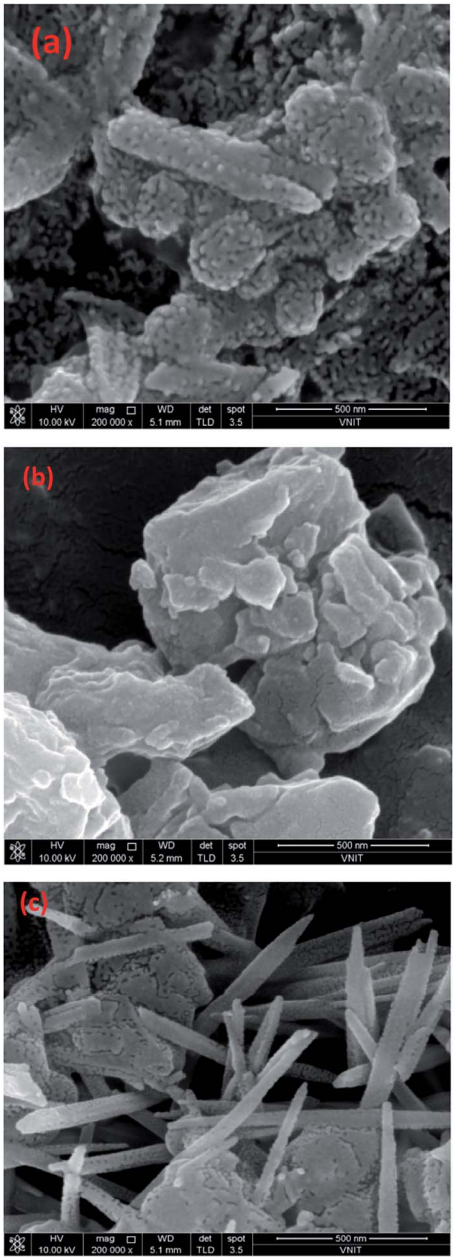


Fig. 4 SEM images of (a) PTh/BQ-MS, (b) PTh/BQ-US (c) PTh/BQ-MW.

The HOMO and LUMO orbitals were observed to be highly delocalized in case of PTh/BQ-MS/US, Fig. 3(a), which confirmed high extent of spatial overlap between the two orbitals. This would result in the reduction of the band gap, and facilitate the charge injection of electrons into the LUMO or holes into the HOMO orbitals. The HOMO–LUMO band gap for PTh/BQ-MS/US was calculated to be 3.21 eV, while it was found to be 2.15 eV for PTh/BQ-MW, Fig. 3(b). The band gap is found to be low for the PTh/BQ-MW oligomer due to the presence of carbonyl linkages that facilitate the charge transfer through the chain.

## Morphological analysis

The SEM of PTH/BQ-MS, Fig. 4(a), reveals a sea coral-like morphology, comprising of elongated agglomerates of bright particles, associated with PTh, while the dark particles are correlated to the BQ. The morphology of PTh/BQ-US, Fig. 4(b), exhibits a spherical cluster of highly dense bright particles, while the SEM of PTh/BQ-MW, Fig. 4(c), shows formation of rod shaped structures of uniform length.

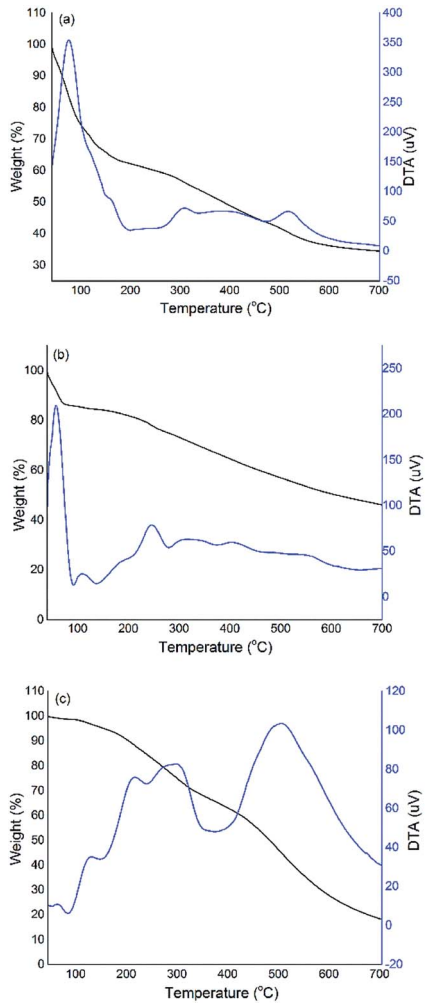


Fig. 5 TGA profiles of (a) PTh/BQ-MS, (b) PTh/BQ-US (c) PTh/BQ-MW.

## Thermal analysis

The thermal stability of PTh/BQ-MS, PTH/BQ-US and PTh/BQ-MW was investigated in the temperature range of 35–800 °C as shown in Fig. 5. The oligomer PTH/BQ-MS exhibits a weight loss of 20% in the temperature range of 100–200 °C due to the elimination of moisture, while a sharp endothermic DTA peak is observed around this temperature range. The second decomposition event is observed at 295 °C with total weight loss of 67% due to the dissociation of C=O, C–H, and C–S bonds and random scission within the oligomeric chain and a broad endothermic peak is also observed in the said region. The char residue, noticed at 800 °C is observed to be 33.89%. The TGA-DTA profile of PTh/BQ-US also reveals a sharp decomposition event at 75 °C with a total weight loss of 10%. An intense DTA peak is also found in this range, which is attributed to the loss of water molecules. A small DTA peak is noticed in the temperature range of 250 °C, exhibiting 20% weight loss, while the char residue at 800 °C is noticed to be 41.40% confirming a slightly higher thermal stability of this polymer as compared to others. Interestingly, the TGA-DTA profile of PTh/BQ-MW shows a 20 wt% loss at 200 °C, which is attributed to the decomposition of some branched chains of the oligomer, while almost 30 wt% loss is observed at 300 °C, due to the dissociation of C=O, C–H, and C–S bonds and the random scission within the oligomeric chain. The char content is observed to be 13%, in this case, confirming almost complete degradation of the polymer at 800 °C. Hence, it can be concluded that the thermal stability of the oligomers of PTh/BQ-MS and PTh/BQ-US are observed to be higher than PTH/BQ-MW, which is attributed to the intermolecular hydrogen bonding due to the conversion of benzoquinone to hydroquinone, while in the case of PTH/BQ-MW, a steep decomposition profile is obtained and the oligomer shows a relatively fair thermal stability up to 300 °C,

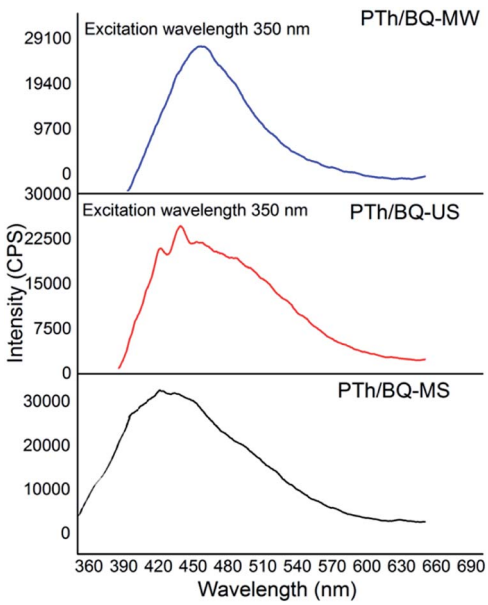


Fig. 6 Fluorescence emission spectra of PTh/BQ synthesized by different methods.

Table 2 Fluorescence and singlet oxygen quantum yield values of PTh/BQ

| | | | | Singlet oxygen values | |
|---|---|---|---|---|---|
| Polymer | Peak position | Integrated peak area | Quantum yield ($\Phi$) | Rate constant ($k_r$) $s^{-1}$ | Quantum yield ($\Phi$) |
| PTh/BQ-MS | 425 | $1.45 \times 10^7$ | 0.0094 | $4.280 \times 10^{-4}$ | 0.013 |
| PTh/BQ-US | 430 | $1.23 \times 10^6$ | 0.014 | $9.877 \times 10^{-4}$ | 0.014 |
| PTh/BQ-MW | 450 | $1.88 \times 10^6$ | 0.024 | $1.38 \times 10^{-3}$ | 0.304 |

beyond which the decomposition is observed to be rapid, leaving about hardly 13% residue at 800 °C.

### Fluorescence emission and confocal studies

Upon excitation at 350 nm, the fluorescence emission spectrum of PTh/BQ/MS, Fig. (6), reveals a broad and pronounced peak at 420 nm, while for PTh/BQ-US, the peak is noticed at 425 nm. Both of the peaks correspond to the $S_1 \rightarrow S_0$ transition. The emission spectrum of PTh/BQ/MS exhibits a broad and intense peak at 450 nm, and its intensity is found to be higher compared to peaks observed in case PTh/BQ-MS and PTh/BQ-US. The quantum yields ($\Phi$) were calculated as per the reported method by using Rhodamine B as a reference.[13–15].

The $\Phi$ values were obtained as 0.0094, 0.014 and 0.024 respectively for PTh/BQ/MS, PTh/BQ/US and PTh/BQ/MW, Table 2.

The confocal image of PTH/BQ-MS, Fig. 7(a), reveals a weak emission in the red region, while the confocal image of PTH/BQ-US, Fig. 7(b), shows intense red agglomerated particles. Interestingly, the confocal image of PTh/BQ-MW, Fig. 7(c), displays scattered tiny red particles and the intensity of the red emission is observed to be higher than the other two oligomers. Hence, it can be concluded that the microwave-assisted Suzuki method, significantly improved the fluorescence emission as well as the intensity of the emission in the red region.

### Singlet oxygen generation studies

The $^1O_2$ generation of polymers in ethanolic solution was investigated under a red laser light irradiation which was measured by using 1,3-diphenylisobenzofuran (DPBF) as a $^1O_2$ quencher. The absorbance peak of DPBF at ~410 nm unusually decreases within 1 min in the presence of polymers under red laser light ($\lambda = 650$ nm), suggesting $^1O_2$ generation (given in ESI as Fig. S2(a–d)).†

The PTh/BQ-MW exhibits considerably higher $^1O_2$ generation efficiency than PTh/BQ-MS and PTh/BQ-US, Fig. 8(a) and (b). The kinetics plot reveals the fact that the $k$ values were obtained as 0.00138 $s^{-1}$, $4.280 \times 10^{-4}$ $s^{-1}$ and $9.877 \times 10^{-4}$ $s^{-1}$ for PTh/BQ-MS, PTh/BQ-US and PTh/BQ-MW respectively, Table 2. The highest $k$ value is obtained for PTh/BQ-US. The $^1O_2$ quantum

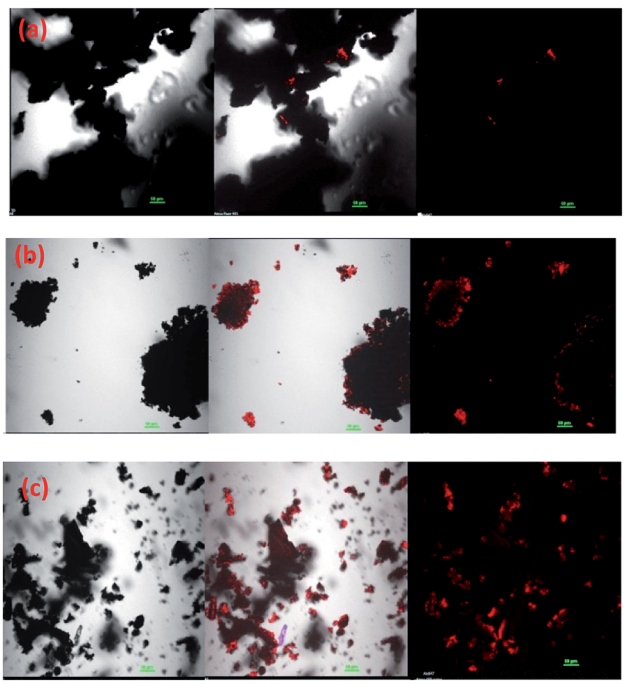


Fig. 7 Confocal images of (a) PTh/BQ-MS (b) PTh/BQ-US, (c) PTh/BQ-MW.

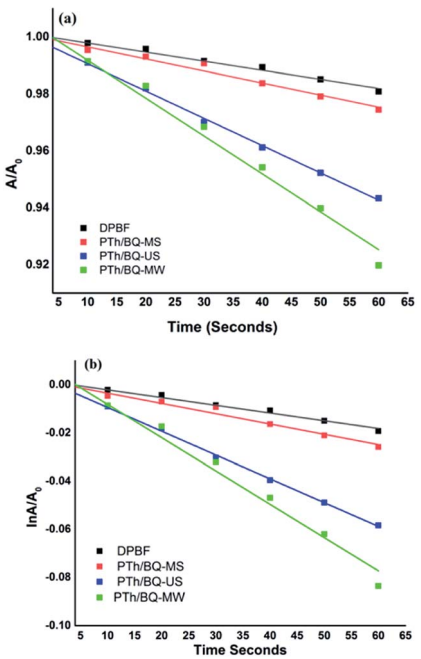


Fig. 8 Singlet oxygen generation plot of (a) $A/A_0$ *vs.* time (b) ln $A/A_0$ *vs.* time.

yield ($\Phi$) for PTh/BQ-MW was found to be ~0.30, which was found to be higher than PTh/BQ-MS, PTh/BQ-US.

## Conclusion

Co-oligomers of thiophene with benzoquinone were successfully synthesized by magnetic stirring, ultrasonication and microwave irradiation. IR analysis confirmed the formation of hydroquinone incorporated PTh *via* magnetic stirring, ultrasonication, while the formation of benzoquinone-incorporated PTh, took place *via* microwave irradiation. The structures observed were in agreement with the theoretical FTIR. Similarly, UV-visible studies supported the formation of hydroquinone-based PTh, obtained *via* magnetic stirring, ultrasonication, which was found to be in agreement with the theoretical UV spectra. The band gap values for PTh/BQ-MW were found to be lower than that of PTh/BQ-MS and PTh/BQ/US. The morphology was found to be self-assembled for PTh/BQ-MW, showing the formation of uniform rods. The thermal stability of PTh/BQ-MS and PTh/BQ/US was found to be higher than PTh/BQ-MW. The fluorescence studies revealed intense emission around 450 nm upon excitation at 350 nm, while the confocal images showed intense signal for PTh/BQ-MW as well as high $^1O_2$ generation and could therefore be utilized as an effective fluorescence imaging agent in photodynamic therapy.

## Conflicts of interest

There are no conflicts to declare.

## Acknowledgements

The author Neetika Singh acknowledges RGNF-SRF UGC, India for providing funding support to conduct this research work.

## References

1 L. Zhang, B. Wang, X. Li, G. Xu, S. Dou, X. Zhang, X. Chen, J. Zhao, K. Zhang and Y. Li, Further understanding of the mechanisms of electrochromic devices with variable infrared emissivity based on polyaniline conducting polymers, *J. Mater. Chem. C*, 2019, **7**, 9878–9891.

2 M. Heydari Gharahcheshmeh and K. K. Gleason, Device Fabrication Based on Oxidative Chemical Vapor Deposition (oCVD) Synthesis of Conducting Polymers and Related Conjugated Organic Materials, *Adv. Mater. Interfaces*, 2019, **6**, 1801564.

3 X. Jia, Y. Ge, L. Shao, C. Wang and G. G. Wallace, Tunable Conducting Polymers: Toward Sustainable and Versatile Batteries, *ACS Sustainable Chem. Eng.*, 2019, **7**, 14321–14340.

4 B. S. Dakshayini, K. R. Reddy, A. Mishra, N. P. Shetti, S. J. Malode, S. Basu, S. Naveen and A. V. Raghu, Role of conducting polymer and metal oxide-based hybrids for applications in ampereometric sensors and biosensors, *Microchem. J.*, 2019, **147**, 7–24.

5 X. Hu, X. Meng, L. Zhang, Y. Zhang, Z. Cai, Z. Huang, M. Su, Y. Wang, M. Li, F. Li, X. Yao, F. Wang, W. Ma, Y. Chen and Y. Song, A Mechanically Robust Conducting Polymer Network Electrode for Efficient Flexible Perovskite Solar Cells, *Joule*, 2019, **3**, 2205–2218.

6 T. Nakamura, Y. Ishikura, N. Arakawa, M. Hori, M. Satou, M. Endo, H. Masui, S. Fuse, T. Takahashi, Y. Murata, R. Murdey and A. Wakamiya, Donor–acceptor polymers containing thiazole-fused benzothiadiazole acceptor units for organic solar cells, *RSC Adv.*, 2019, **9**, 7107–7114.

7 A. O. Pati, D. Y. Curtin and I. C. Paul, *J. Am. Chem. Soc.*, 1984, **106**, 348.

8 M. Catellani, S. Luzzati, N.-O. Lupsac, R. Mendichi, R. Consonni, A. Famulari, S. V. Meille, F. Giacalone, J. L. Segura and N. Martín, Donor–acceptor polythiophene copolymers with tunable acceptor content for photoelectric conversion devices, *J. Mater. Chem.*, 2004, **14**, 67–74.

9 J. Li, W. Shi, J. Zhang and I. Nurulla, p-Benzoquinone diimines and thiophene based alternating copolymers: organometallic catalyzed syntheses and elementary characterization, *J. Polym. Res.*, 2012, **19**, 9739.

10 J. Grimshaw and S. D. Perera, Electrochemical behaviour of poly(thiophene-benzoquinone) films, *J. Electroanal. Chem. Interfacial Electrochem.*, 1990, **278**, 287–294.

11 K. Shiraishi and T. Yamamoto, Synthesis and Electrochemical Properties of New Main Chain Type Polyquinones Constituted of Thiophene-Fused Benzoquinone and Transformation of the Polymers to a Dicyanoquinonediimine Type Polymer, *Polym. J.*, 2002, **34**, 727–735.

12 T. Yamamoto and H. Etori, Poly(anthraquinone)s Having a. pi.-Conjugation System along the Main Chain. Synthesis by Organometallic Polycondensation, Redox Behavior, and Optical Properties, *Macromolecules*, 1995, **28**, 3371–3379.

13 N. singh, P. Kumar, R. Kumar and U. Riaz, Ultrasound–assisted Polymerization of Dyes with Phenylenediamines: A Facile method to Design Polymeric Photosensitizers with Enhanced Singlet Oxygen Generation Characteristics and Anti-Cancer Activity, *Ind. Eng. Chem. Res.*, 2019, **58**, 14044–14057.

14 N. Singh, S. Singh, S. M. Ashraf and U. Riaz, Experimental and theoretical studies of benzoquinone modified poly(ortho-phenylenediamine): singlet oxygen generating oligomers, *Colloid Polym. Sci.*, 2020, **298**, 1443–1453.

15 U. Riaz, N. Singh and P. Kumar, Ultrasound-assisted synthesis of fluorescent oligomers of triphenylamine modified polyquinones: a comparison of experimental and computational spectral studies, *J. Mol. Struct.*, 2020, **1217**, 128374.

 